Downloaded from orbit.dtu.dk on: Jun 29, 2022

DTU Library

Comparison of the Performance of Chilled Beam with Swirl Jet and Diffuse Ceiling Air Supply: Impact of Heat Load Distribution

Bertheussen, Bård ; Mustakallio, Panu ; Kosonen, Risto ; Melikov, Arsen Krikor

Published in:
Proceedings of 11th REHVA World Congress and the 8th International Conference on Indoor Air Quality, Ventilation and Energy Conservation in Buildings

Publication date:
2013

Link back to DTU Orbit

Citation (APA):
Bertheussen, B., Mustakallio, P., Kosonen, R., & Melikov, A. K. (2013). Comparison of the Performance of Chilled Beam with Swirl Jet and Diffuse Ceiling Air Supply: Impact of Heat Load Distribution. In *Proceedings of 11th REHVA World Congress and the 8th International Conference on Indoor Air Quality, Ventilation and Energy Conservation in Buildings* [Paper ID: 29]

General rights
Copyright and moral rights for the publications made accessible in the public portal are retained by the authors and/or other copyright owners and it is a condition of accessing publications that users recognise and abide by the legal requirements associated with these rights.

- Users may download and print one copy of any publication from the public portal for the purpose of private study or research.
- You may not further distribute the material or use it for any profit-making activity or commercial gain
- You may freely distribute the URL identifying the publication in the public portal

If you believe that this document breaches copyright please contact us providing details, and we will remove access to the work immediately and investigate your claim.

Comparison of the Performance of Chilled Beam with Swirl Jet and Diffuse Ceiling Air Supply: Impact of Heat Load Distribution

Bård Bertheussen[1,4], Panu Mustakallio[2], Risto Kosonen[2,3], Arsen Melikov[4]

[1,4]*Erichsen & Horgen A/S, Nydalsveien 36, 0483 Oslo, Norway,*

[1]*BBE@erichsen-horgen.no*

[2]*Halton Oy, Esterinportti 2, 00240 Helsinki, Finland,*
[2]*panu.mustakallio@halton.com,*

[2,3]*Aalto University, Finland; School of Engineering, Department of Energy Technology, Heating Ventilating and Air-Conditioning,* [2]*risto.kosonen@halton.com*

[4]*International Center for Indoor Environment and Energy, Department of Civil Engineering, Technical University of Denmark,* [4]*akm@byg.dtu.dk*

Abstract

The impact of heat load strength and positioning on the indoor environment generated by diffuse ceiling air supply and chilled beam with radial swirl jet was studied and compared. An office room with two persons and a meeting room with six persons were simulated in a test room (4.5 x 3.95 x 3.5 m^3 (L x W x H)). A window (6.5 m^2) was simulated by radiant panels. Four chilled beam units were installed symmetrically on the suspended ceiling together with two exhaust vents. The diffuse ceiling inlet was made of standard perforated acoustic tiles (0.5% total degree of perforation). The room air temperature was controlled at 24 °C. The quality of the generated indoor environment as defined in ISO standard 7730 (2005) was assessed based on comprehensive physical measurements. The systems created Category A thermal environment in cooling situations at heat load of 50 $W \cdot m^{-2}$ and 78 $W \cdot m^{-2}$ (office room) and Category B thermal environment in the meeting room at high heat load of 94 $W \cdot m^{-2}$. The air distribution pattern was influenced by the convective flows from the heat sources. The maximum local velocity in the occupied zone was 0.23–0.26 $m \cdot s^{-1}$. The diffuse ceiling supply did not ensure complete mixing (ventilation effectiveness of 0.4) and the air flow rate had to be above minimum to safeguard the indoor air quality. The radial swirl jet of chilled beam also was not capable of creating complete mixing at high and concentrated heat load (ventilation effectiveness of 0.7).

Keywords – diffuse ceiling air supply, chilled beams, air distribution

1. Introduction

Room air conditioning in office buildings with the use of active chilled beam systems has become popular during the recent years due to the system's ability to remove heat more energy efficiently than all-air systems and more efficient space utilization due to smaller ventilation shafts and ducts since cooling is mainly supplied to the space by water as heat transfer

medium. Chilled beam with radial swirl jet has been introduced with the benefit of more efficient mixing of supply air and the room air. Swirl air diffusion leads to fast decrease of the supply air velocity and increase of its temperature before it reaches the occupied zone. Convection flows generated by internal and external heat gains may significantly affect the air distribution in rooms with active chilled beams [1–2]. The thermal plume from high concentrated heat gains may deflect the jet and increase the velocities in the opposite side of the room [3]. The air distribution and performance of chilled beams with radial swirl flow jet has not been studied and reported in the literature.

Diffuse ceiling air supply is a novel room air distribution system in comfort ventilation. Recently the system has been applied in several office buildings in Denmark and in a classroom in The Netherlands. There are only limited studies on the air distribution in rooms with diffuse ceiling air supply reported in the literature [4–7]. A study by Nielsen *et al.* [4] concludes that diffuse ceiling air supply has superior cooling capacity compared to mixing ventilation, displacement ventilation and low-impulse vertical ventilation.

This paper presents results on the impact of heat load distribution and strength on the air distribution and the indoor environment generated in rooms with chilled beam with swirl jet and diffuse ceiling air supply. Only part of the collected and analyzed results is presented in this paper.

2. Methods

Experimental Facilities

A full-scale test room (L x W x H = 4.5 m x 3.95 m x 3.5 m) was used to simulate both an office and a meeting room. A suspended system ceiling made of acoustic mineral wool tiles was mounted at height 2.7 m. Three fluorescent lighting fixtures were installed suspended below the ceiling. Four chilled beam units with radial swirl diffuser of type Halton CSW (Fig. 1c) were installed symmetrically and recessed into the suspended ceiling together with two extract vents. The wall and ceiling of the void above the suspended ceiling was carefully sealed with a plastic membrane, and air supply ducts were installed with bends facing upwards to pressurize the void and ensure even distribution of air when the void works as plenum for diffuse ceiling air supply (Fig. 1a). The mineral wool tiles were perforated with tubes with an inner diameter of 13.8 mm, constituting a total degree of perforation 0.5% (Fig. 1b).

a) b) c)

Figure 1: a) Plenum (ceiling void) of diffuse ceiling air supply. b) Air distribution principle of diffuse ceiling air supply [4]. c) Air distribution principle of chilled beam with swirl jet [8].

Heat Load Simulators

One of the occupants was simulated by a thermal manikin representing an average female body size. The remaining occupants were simulated with dummies, comprised of head, torso and legs, which were heated by internally installed light bulbs and fans to ensure an even surface temperature. Computers were simulated by light bulbs installed inside metal boxes with output control. A window with area of 6.5 m^2 was simulated by radiation panels using warm water circulation to achieve the surface temperature corresponding to a fixed heat gain. To simulate the effect of direct solar radiation through the window an electric foil with output power control was placed on the floor covering the floor area from the window wall to a distance of 0.8 m.

Experimental Conditions

Eight experiments were performed with the chilled beam with swirl diffuser (CSW) and diffuse ceiling air supply (DC) at different heat load in the room as specified in Table 1. In the case of meeting room asymmetrical heat load distribution was studied as well (case "DC meeting room asymmetrical 94 $W \cdot m^{-2}$"and case "CSW meeting room asymmetrical 94 $W \cdot m^{-2}$", Table 1).

The simulations represent summer conditions and the room temperature was maintained at 24.0±0.5 °C (the room temperature was defined as the average temperature at 1.1 m in 16/20 locations (Figs. 2–3) in the occupied zone).

Chilled water was supplied to the active chilled beam system and the water flow rate and the water temperature was designed to supplement the cooling capacity to the supplied air in respect to the heat load in the experiments.

Table 1: Experimental conditions.

Case	Air flow rate [L·s^{-1}·m^{-2}]	Air supply temp. [°C]	Window surface temp. [°C]
DC office 50 W·m^{-2}	5.2	14.5	26.5±0.5
CSW office 50 W·m^{-2}	2.0	17.9	26.5±0.5
DC office 78 W·m^{-2}	7.7	14.7	32.2±0.5
CSW office 78 W·m^{-2}	2.0	15.7	32.2±0.5
DC meeting room 94 W·m^{-2}	9.4	14.0	32.2±0.5
CSW meeting room 94 W·m^{-2}	4.0	14.3	32.2±0.5
DC meeting room asymmetrical 94 W·m^{-2}	9.5	14.6	32.2±0.5
CSW meeting room asymmetrical 94 W·m^{-2}	4.0	14.2	32.2±0.5

The heat load is specified in Table 2. The layout in the office cases at 50 W·m^{-2} and 78 W·m^{-2} was identical. These simulations represent an office with two workplaces in summer situation with moderate and high heat load (Fig. 2). The conditions in the meeting room cases simulated summer season and six seated persons (Fig. 3), with high internal and external loads (Table 2). The cases "DC/CSW meeting room asymmetrical 94 W·m^{-2}" were studied with unchanged heat load but rearranged distribution. In these cases all the occupants were placed on the same side of the table simulating two rows of tree persons watching a presentation.

Table 2: Heat gains in the simulations.

Heat gain	Office 50 W·m^{-2} [W]	Office 78 W·m^{-2} [W]	Meeting room 94 W·m^{-2} [W]
Persons (manikins)	75	75	75
Persons (dummies)	83	83	5x83
Lighting fixtures	2x2x36	2x2x36	2x2x36
Lighting fixtures	2x58	2x58	2x58
Computers	2x178	2x178	2x153
Window	114	426	426
Solar load (on floor)	0	189	189
Total load	888	1389	1671

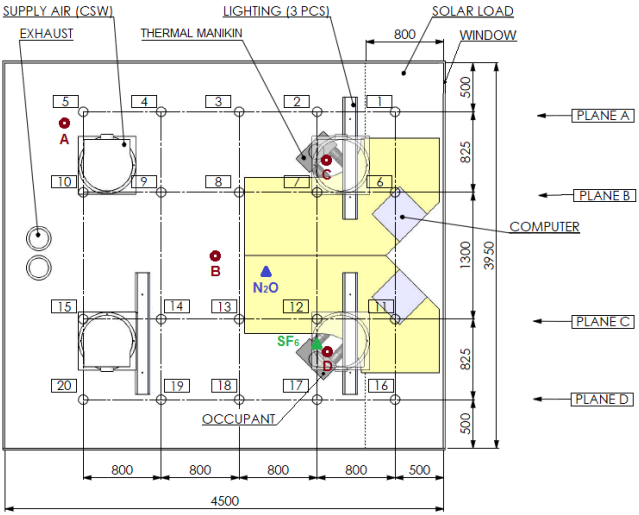

Figure 2: Experimental set up case "DC/CSW office 50 W·m^{-2}" and case "DC/CSW/ office 78 W·m^{-2}". Mean air speed and mean air temperature measured in locations numbered from 1–20 (locations 6, 7, 11 and 12 excluded). Concentration of tracers gases measured in locations A–D (heights: A: 0.1, 0.6, 1.1, 1.7, 2.4 m, B: 0.1, 0.6, 1.1, 1.7, 2.4 m, C–D: 1.1 m).

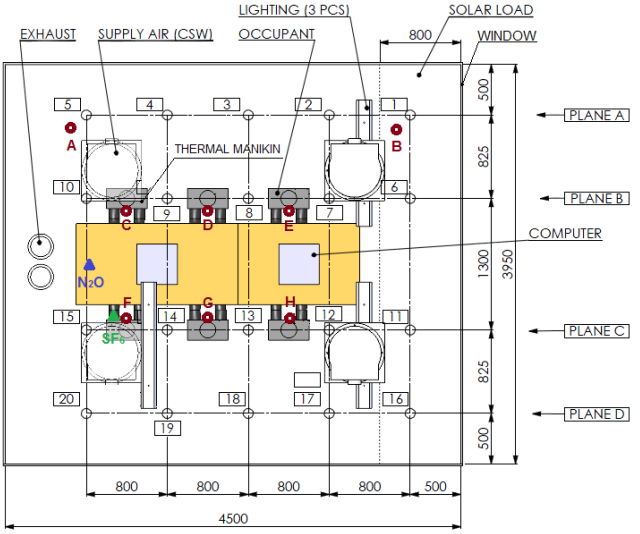

Figure 3: Experimental set up case "DC/CSW meeting room 94 W·m^{-2}". Mean air speed and mean air temperature measured in locations numbered from 1–20. Concentration of tracers gases measured in locations A–H (heights: A: 0.1, 1.1, 1.7 m, B: 0.1, 1.1, 1.7 m, C–H: 1.1 m).

Measuring Procedure

Measurements of air speed and air temperature were conducted in several locations in the occupied zone to evaluate the velocity conditions, draught rate and temperature distribution (vertical temperature difference and non-uniformity in the temperature distribution). The air speed and air temperature was measured in six heights (0.1, 0.2, 0.5, 1.1, 1.5, 1.8 m) above the floor level at twenty locations positioned symmetrically in a grid as shown in Figs. 2–3. The measurements were initiated when the room conditions became stabile. Three minutes mean values for the air speed and air temperature, in addition to the turbulence intensity, were obtained from each position. When the measurements in one of the locations (x, y) finished, the stand with the sensors was moved to the next location. A waiting time of three minutes was introduced after the stand was moved to another position before the next series of measurements were initiated.

Smoke was released into the supply to visualize the air flow pattern in the room. Smoke visualization was performed in each of the experiments and this part of the experiment was recorded by a digital video camera.

Tracer gas measurements were conducted in the experiments for the purpose of evaluating the ventilation effectiveness of the systems investigated and normalized concentration of pollution in the room. Sulfur hexafluoride (SF_6) was used to simulate an active source of contamination (combined heat source and contaminant source) in this case the biofluents emitted from a human being. The SF_6 was released from the torso of one of occupants in the experiments. Nitrous oxide (N_2O) was used to simulate emissions from a passive source represented by emissions from a table. The tracer gas was released as a constant dose (0.15 $l \cdot s^{-1}$) through a sponge fastened to the source to prevent high momentum of the released tracer gas flow. The points of release are indicated on Figs. 2–3. The tracer gas concentrations in the room were allowed to reach steady state conditions before the concentration measurements were initiated. Air was sampled through tubes from several points in the room and from the supply and return ducts, and the concentrations of SF_6 and N_2O were monitored. The measurement locations and points are defined in Figs. 2–3. When the concentrations reached stable values, thus steady state conditions, the necessary number of measurement were conducted to obtain sufficient number of concentration values from each channel to allow for statistical analysis of the results (8–20 values). The arithmetic mean was calculated from the obtained values in each point and the mean values were used in the analysis to calculate ventilation effectiveness.

Measuring Equipment

The air speed was measured using a multichannel low Velocity Thermal Anemometer (Measurements System HT-400, manufactured by “Sensor”),

consisting of six transducer units HT-426-0 with omnidirectional velocity probes type HT-412. The velocity measurement range of the instrument is 0.05–5 $m \cdot s^{-1}$. The air temperature was measured using six Pt100 Class A sensors positioned close to each velocity probe. The systems were interfaced a computer for the purpose of data collection.

The air flow rates in the supply and return ducts were measured with two Furness Controls FCO33 (Orifice plate according ISO 5167 with differential pressure transmitter). The total water flow rate to the CSW chilled beams was measured with Krohne Electromagnetic flow meter IFC 010. These two systems were interfaced a computer for the purpose of data collection.

The concentration of tracer gases were monitored by a Brüel & Kjær Photoacoustic Multi Gas Analyzer—Model 1302; repeatability 1% of the measured value. Purpose built sampler and dozer with software were used to dose the tracer gases (0.15 $L \cdot s^{-1}$) and to collect the air samples for the photoacoustic multi gas analyzer.

The ventilation system had a built in smoke machine (F-100 Performance fog generator, High End Systems, USA) which was used to release smoke into the supply to visualize the air distribution from the air terminal device.

Data analyses

The measured data were used to evaluate the thermal environment according to the categories specified in ISO standard 7730 (2005). Ventilation effectiveness, defined as the tracer gas concentration in the exhaust divided by the tracer gas concentration at the measured points in the room, was used to assess the air quality in the room as generated by the systems.

3. Results and discussion

The effect of the heat load distribution on the air distribution was studied in 8 cases. The office simulations introduced a highly asymmetrical heat load distribution where all the heat gains were positioned on one side of the room, i.e. the side of the window wall. The meeting room simulations introduced a more uniform heat load distribution and the occupants and the computers were distributed evenly in the room.

In the office room simulations the main effect of the highly asymmetrical heat loads arrangement on the air flow pattern was circulation in the whole room (revealed by the smoke visualizations) which led to high air speeds in the lower part of the occupied zone opposite to the heat gains (Fig. 4). The main air flow pattern looked very similar at moderate and high heat loads. However, the maximum air speed in the occupied zone increased substantially in the case CSW from 0.18 $m \cdot s^{-1}$ at 50 $W \cdot m^{-2}$ to 0.26 $m \cdot s^{-1}$ at

78 W·m^{-2} and in the case DC from 0.20 m·s^{-1} at 50 W·m^{-2} to 0.23 m·s^{-1} when the heat load was increased to 78 W·m^{-2}. The thermal environment for the occupants in the office simulations was not noticeable affected by the increased heat load. Both systems created uniform thermal environment in the area of the occupants with mean air speeds generally in the range 0.05–0.1 m·s^{-1} in all the office simulations. ISO 7730 (2005) defines draught rate index of maximum 10% to satisfy the draught requirements for Category A thermal environment. None of the locations in the occupied side of the office room had draught rate index above 10%.

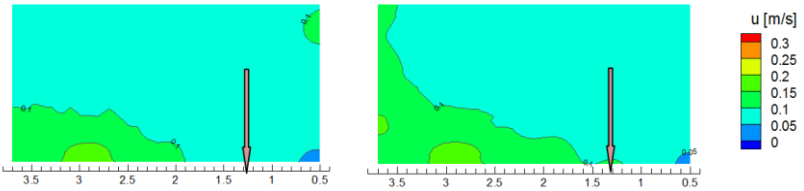

a) Case DC office 50 W·m^{-2}: Plane A b) Case CSW office 50 W·m^{-2}: Plane A

Figure 4: Examples of air speed distribution in office room. The x-axis on the figures shows the longitudinal position in the room and the air speed was measured at x = 3.7, 2.9, 2.1, 1.3, 0.5 m from the window. The planes cover the area from 0.1 to 1.8 m above floor level. The positions of the planes are defined in Figs. 2–3. Plane A is in the boundary of the occupied zone. The position of the occupant (manikin) is indicated with red arrow.

In the case of meeting room the uniform distribution of occupants and computers in case DC (94 W·m^{-2}) and case CSW (94 W·m^{-2}) created generally higher air speeds in the occupied zone when compared to the office room simulations. Air circulation could be observed in the room in the opposite side of the heat loads. The maximum air speed in case CSW (94 W·m^{-2}) was 0.22 m·s^{-1}, i.e. 0.04 m·s^{-1} lower compared with case CSW office room at 78 W·m^{-2}. The maximum air speed in case DC (94 W·m^{-2}) was 0.22 m·s^{-1}, i.e. almost identical with case "DC office 78 W·m^{-2}". Several of the locations in the vicinity of the occupants in the meeting room had draught rate index in the range 11–20% which corresponds to Category B thermal environment in ISO 7730 (2005).

When all the occupants in the meeting room were moved to one side of the table (asymmetrical location of heat load) the air circulation in the cases CSW and DC (94 W·m^{-2}) caused by the external heat gains was interrupted by the perpendicular convective flows from the occupants and computers, resulting in reduced velocities and reduced draught rate index in the area of the occupants. In fact the quality of the thermal environment was slightly improved.

The impact of the airflow pattern on the distribution of pollution in the room was assessed by the ventilation effectiveness in the breathing zone of

the occupants. Effectiveness in removing contamination from active (SF_6) and passive (N_2O) pollution sources was assessed. Tracer gas measurements were not conducted in the case "CSW office room 78 $W \cdot m^{-2}$" and the case "CSW meeting room 94 $W \cdot m^{-2}$" due to problems with the experimental facilities at the beginning of the experiment.

The results presented in Fig. 5 show that the CSW chilled beam system achieved good mixing in the case "CSW office 50 $W \cdot m^{-2}$" with ventilation effectiveness equal to approximately 1 (the ventilation effectiveness was defined as tracer gas concentration measured at the exhaust divided by the tracer gas concentration at the measured point). The system was not able to create complete mixing in case of meeting room with asymmetrical heat load (94 $W \cdot m^{-2}$); the ventilation effectiveness was 0.7 for N_2O. These results imply that the desired indoor air quality may be safeguarded by the system at outdoor air flow rate equal to the minimum ventilation rate when the heat load is moderate, and that higher air flow rates are required when the heat load is increased.

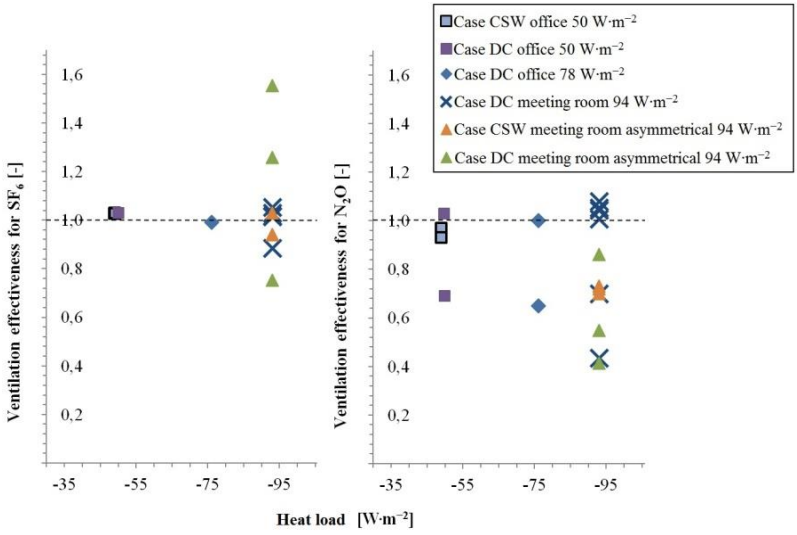

a) SF_6 (combined heat source) b) N_2O (passive source)

Figure 5: Ventilation effectiveness in the breathing zone of the occupants (Figs. 2–3). y-xasis: ventilation effectiveness, x-axis: heat load.

Complete mixing was not achieved in any of the experiments with diffuse ceiling air supply. The ventilation effectiveness was as low as 0.4 for N_2O in case "DC meeting room 94 $W \cdot m^{-2}$" and case "DC meeting room asymmetrical 94 $W \cdot m^{-2}$" (Fig. 5). The results in Fig. 5 also show that the

ventilation effectiveness decrease with increased heat load. The results imply that minimum ventilation rates cannot be used with the system.

4. Conclusions

The two systems were able to generated high quality of thermal environment at heat load up to 78 $W \cdot m^{-2}$ and medium quality at heat load of 94 $W \cdot m^{-2}$, respectively Category A and Category B according to ISO Standard 7730 (2005).

The ventilation effectiveness in the case of CSW chilled beam system was higher than the ventilation effectiveness obtained with diffuse ceiling system. In the case of CSW the ventilation effectiveness decreased with the increase of the heat load (from 1 to 0.7 at 94 $W \cdot m^{-2}$). The ventilation effectiveness with the diffuse ceiling system was low (0.4 under the studied conditions), i.e. low inhaled air quality may be expected.

The air distribution of diffuse ceiling air supply and CSW chilled beam system is affected by to natural convection flows and asymmetrical heat loads arrangement may cause circulation and high velocities in the opposite side of the room of the heat sources. The systems may create stagnant zones with polluted air. Outdoor air flow rate higher than the required is needed to safeguard the desired indoor air quality.

5. References

[1] Koskela H., Häggblom H., Kosonen R., Ruponen M., (2010) "Air Distribution in an Office Environment With Asymmetric Workstation Layout Using Chilled Beams", *Building and Environment*, Vol. 45, Iss: 9, pp. 1923–1931.

[2] Kosonen R., Melikov A. K., Yordanova B., Bozkhov L., (2007) "Impact of Heat Load Distribution and Strength on Airflow Pattern in Rooms with Exposed Chilled Beams", *Proceedings: Roomvent 2007*, Helsinki Finland, 13–15 June 2007.

[3] *Zboril V., Melikov A. K, Yordanova B., Bozkhov L., Kosonen R., (2007) "Airflow Distribution in Rooms with Active Chilled Beams", Proceedings: Roomvent 2007, Helsinki Finland, 13–15 June 2007.*

[4] Nielsen P. V., Jakubowska E., (2009) "The Performance of Diffuse Ceiling Inlet and other Room Air Distribution Systems". *Proceedings: Cold Climate HVAC 2009*, Sisimiut Greenland, 16–19 March 2009.

[5] Jacobs P., Oeffelen E. C. M., Knoll B., (2008) "Diffuse Ceiling Ventilation, a New Concept for Healthy and Productive Classrooms". *Proceedings: Indoor Air 2008*, Copenhagen Denmark, 17–22 August 2008.

[6] Nielsen P. V., Jensen L. R., Rong L., (2010) "Diffuse Ceiling Inlet Systems and the Room Air Distribution", *Proceedings: Clima 2010 - REHVA World Congress*, Antalya Turkey, 9–12 May 2010.

[7] Nielsen P. V., Jensen L. R., Holberg-Jørgensen P., (2010) "Diffus loftsindblæsning—fra laboratoriefosøg til praktisk anvendelse". HVAC Magasinet, Iss: 10, pp. 50–55, 2010.

[8] Virta M., ed. (2007) *Chilled Beam Application Guidebook*, 2nd ed., Rehva Federation of European Heating and Air-conditioning Associations, Brussels.